

****TITLE****

*ASP Conference Series, Vol. **VOLUME**, **PUBLICATION YEAR***

****EDITORS****

First detection of Zeeman splitting of water masers in circumstellar shells

Wouter Vlemmings

Sterrewacht Leiden, Postbus 9513, 2300 RA Leiden, The Netherlands

Phil Diamond

Jodrell bank Observatory, University of Manchester, Macclesfield, Cheshire, SK11 9DL, England

Huib Jan van Langevelde

Joint Institute for VLBI in Europe, Postbus 2, 7990 AA, Dwingeloo, The Netherlands

Abstract. The strength and structure of the magnetic fields in circumstellar envelopes have been measured through polarization observations of OH and SiO masers. Here we present the first results obtained by observing the circular polarization of the H₂O masers using VLBI. SiO masers are probes of the high temperature and density regime close to the central star. OH masers are found at much lower densities and temperatures, generally much further out in the circumstellar envelope. The detection of the Zeeman splitting of the (6₁₆-5₂₃) rotational transition of the H₂O maser allows us to determine the magnetic field strength in the intermediate temperature and density regime.

1. Introduction

Masers are excellent probes of the dynamics and kinematics of the circumstellar envelope (CSE) of late type stars. Maser polarization observations have revealed the strength and structure of the magnetic field throughout the CSE. Observations of SiO maser polarization have shown highly ordered magnetic fields of ≈ 5 -10 G close to the central star, at radii of 5-10 AU (Kemball & Diamond, 1997). At much lower densities and temperatures and generally much further from the star, OH maser observations measure fields of ≈ 1 mG (Szymczak & Cohen, 1997). But for the intermediate region, at distances of a few hundred AU, no information is available. In this region the H₂O maser emission occurs. Since water is a non-paramagnetic molecule, determination of the magnetic field is significantly more difficult. The Zeeman splitting of H₂O is extremely small for the field strengths expected (few hundred mG), only $\approx 10^{-3}$ times the typical Gaussian line width of the H₂O maser line ($\Delta\nu_L \approx 20$ kHz). However, Fiebig & Güsten (1989, hereafter FG) showed that in the presence of such magnetic fields the Zeeman splitting can be detected with high spectral resolution polarization observations.

2. Observations

The observations were performed at the NRAO¹ Very Long baseline Array (VLBA) in December 1998. We observed 4 late type stars (S Per, U Her, VY CMa and NML Cyg), the results presented here are the first results for the supergiant S Per, a source with strong water maser features and relatively simple structure. The stellar velocity V_{LSR} of S Per is -38.5 km s^{-1} . We observed the $6_{16} - 5_{23}$ rotational transition of H_2O at 22.235 GHz. The beam width is $\approx 0.7 \times 0.3 \text{ mas}$. This allows us to resolve the different H_2O maser features in the CSE. The data were correlated twice, once with modest ($7.8 \text{ kHz} = 0.1 \text{ km s}^{-1}$) spectral resolution, which enabled us to generate all 4 polarization combinations (RR, LL, RL and LR). The second correlator run was performed with high spectral resolution ($1.95 \text{ kHz} = 0.027 \text{ km s}^{-1}$), necessary to detect the circular polarization signature of the H_2O Zeeman splitting, and therefore only contained the two polarization combinations RR and LL. The data analysis followed the method of Kembball, Diamond & Cotton (1995). The first calibration steps were performed on the data-set with modest spectral resolution. Using the AIPS package, we started by applying standard amplitude calibration. We then used the maser source to determine the R-L gain ratio. Delay and Phase calibrations were performed on the R-polarization only and then applied to both R and L. A continuum calibrator source was used to determine R-L delay and RR-LL phase offsets. Finally feed polarization calibration was done with the AIPS task SPCAL. The solutions were then applied to the high spectral resolution data-set. The final fringe fitting and self-calibration were performed on a strong maser feature, applying solutions obtained on R to both R and L.

3. Method

Our treatment closely follows the analysis performed by FG. We have included the possibility of multiple masing hyperfine components, assuming the $F = 7 - 6$ hyperfine component to be dominant. Each hyperfine component will split into 3 groups of lines (σ^+ , σ^- and π). For a magnetic field B parallel to the line of sight the Zeeman pattern consists of the two circular polarized σ components only. The right- and left-handed (RR and LL) spectra, corresponding to the σ^\pm components will only be slightly shifted against each other. This corresponds to a characteristic frequency shift of the order of $\Delta\nu_Z \approx 10^3 \text{ Hz} \cdot [B_{\text{Gauss}}]$. As a result, the observed V-spectrum (RR-LL) will be a sine-shaped function, corresponding to the derivative I' of the total power spectrum. The amplitude of this function depends on the maser line width, the magnetic field strength, and on which hyperfine components actually contribute to the maser. By calculating synthetic V-spectra we find a relationship between the magnetic field B and the percentage of circular polarization P_V , shown in Fig. 1a for different hyperfine components and line widths.

¹The National Radio Astronomy Observatory is a facility of the National Science Foundation operated under cooperative agreement by Associated Universities, Inc.

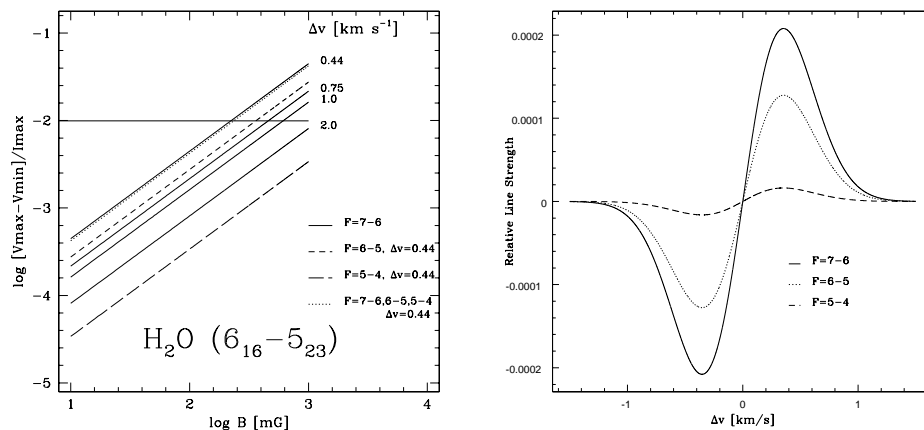


Figure 1. a) $B - P_V$ relation. b) Synthetic V-spectra for an external field of 50 mG and a line width of $\Delta v_L = 0.5$ km s $^{-1}$.

4. Results

A total intensity map of the maser features is shown in Fig. 2a. Fig 2b shows total power and circular polarization spectrum on the strongest feature. From this, we find for the magnetic field strength along the line of sight $B_{\parallel} = 279 \pm 30$ mG. The exact value however, is dependent on which hyperfine component(s) actually contribute to the maser. This value was obtained by using a fitted line strength ratio for the three strongest hyperfine components. Because the V-spectra is negative on the blue shifted side, the observed component B_{\parallel} is pointing away from us.

We have not found any indication of linear polarization, which is consistent with the observations of Barvainis & Deguchi (1989)

5. Discussion

A radiative transfer treatment for the water maser was performed by Nedoluha & Watson (1992). Their treatment did not predict the anti-symmetric shape of the V-spectrum as shown in our observations and those by FG. However, our calibration procedure assumes similar R- and L-polarization line profiles. Thus the observed anti-symmetric shape is a necessary result of our data calibration. The observed V-spectrum however, is not directly proportional to I' , as would have been expected in the simple model. The minimum and maximum of the sine-shaped function are not located at $\pm\sigma/\sqrt{2}$, with σ being the observed Gaussian line width, as seen in Fig. 2b. This narrowing of the V-spectrum can possibly be attributed to the overlap of the multiple hyperfine components, as predicted by the treatment and analysis of NW. Due to this our magnetic field strength can be overestimated by at most a factor of 2.

The magnetic field strength we derive agrees well with previous observations of SiO and OH masers. The dependence of $B \propto r^{-2}$ for a solar-type magnetic field is the most likely. For a dipole medium, the magnetic field is expected

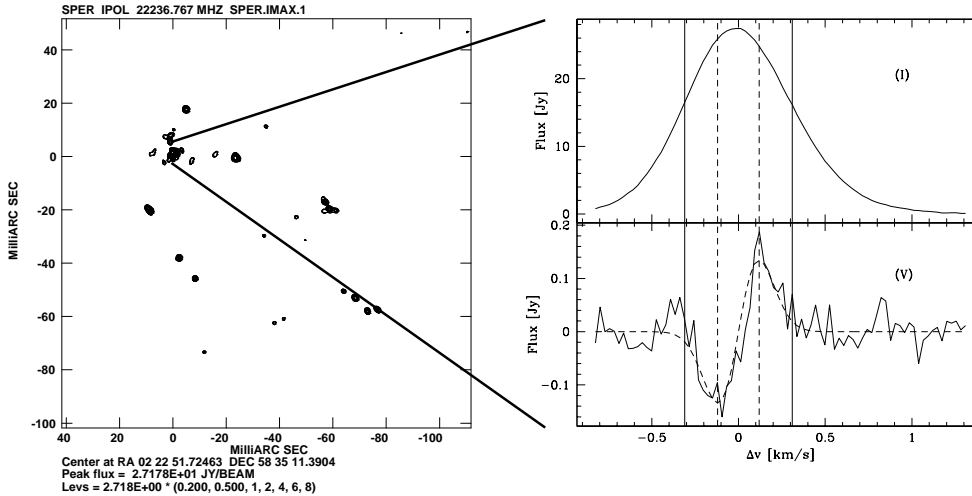


Figure 2. a) Total intensity image of the H₂O maser features around S Per. b) Total power (I) and circular polarization (V) spectrum of the brightest H₂O maser feature around S Per. The dashed line is the fit of the synthetic V -spectrum to the observed spectrum.

to vary with r^{-3} , which appears to be too steep to accurately describe the observations. In S Per, the H₂O and OH masers are observed to exist at similar projected distances (Masheded et al., 1999). This disagrees with the observed differences in the magnetic field strengths, except if the magnetic field could remain frozen in high density clumps.

In conclusion, although the exact influence of the hyperfine interaction is not yet clear, our observations yield a magnetic field strength of $B_{\parallel} = 279 \pm 30$ mG. A more detailed description of the detection of circular polarization presented here can be found in Vlemmings et al. (2001).

Acknowledgments: This project is supported by NWO grant 614-21-007.

References

- Barvainis, R., & Deguchi, S. 1989, *AJ*, 97, 1089
 Fiebig, D., & Güsten, R. 1989, *AA*, 214, 333
 Kemball, A.J., Diamond, P.J., & Cotton, W.D. 1995, *A&AS*, 110, 383
 Kemball, A.J., & Diamond, P.J. 1997, *ApJ*, 481, L111
 Masheded, M.R.W., et al. 1999, *NewAR*, 43, 563
 Nedoluha, G.E., & Watson, W.D. 1992, *ApJ*, 384, 185
 Richards, A.M.S., Yates, J.A., & Cohen, R.J. 1999, *MNRAS*, 306, 954
 Szymczak, M., & Cohen, R.J. 1997, *MNRAS*, 288, 945
 Vlemmings, W.H.T, Diamond, P.J., & Van Langevelde, H.J. 2001, *submitted to A&A*